

# Investigation of the co-crystallisation of N-heterocycles

By

**Leigh-Anne Loots**

*Thesis presented in partial fulfilment of the requirements for the  
degree of Master of Science*



*Stellenbosch University*

Department of Chemistry and Polymer Science

Faculty of Science

Supervisor: Leonard J. Barbour

March 2009

said that the insertion of pyridazine into the array drives the perpendicular arrangement of the catechol molecules.

### $\beta$ -O2N2 (1:2)

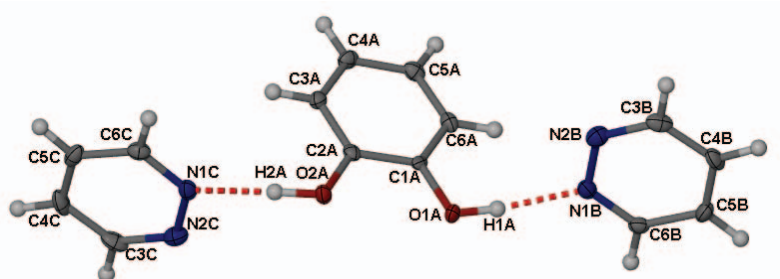
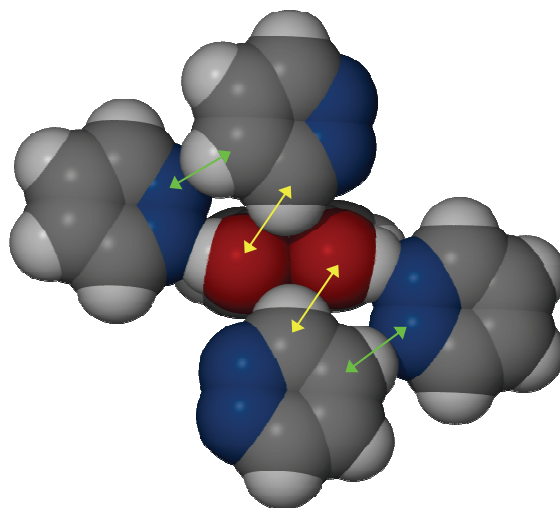
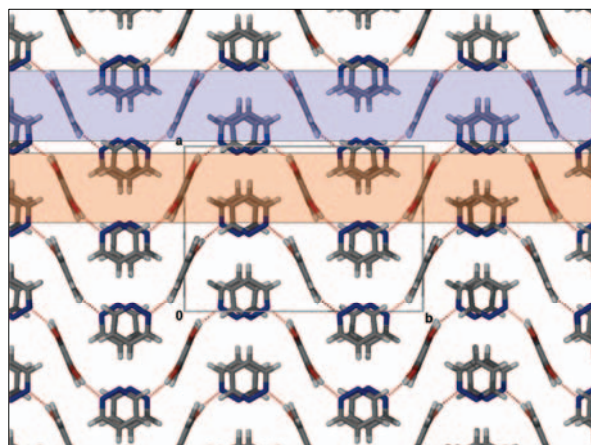


Figure 3.32: 50% probability thermal ellipsoid plot of the ASU of  $\beta$ -O2N2.

The structure of  $\beta$ -O2N2 was ultimately refined as a non-merohedral twinned crystal with the help of Drs. Regine Herbst-Irmer (University of Göttingen, Germany) and Ina Dix (Bruker AXS, Karlsruhe, Germany). The ASU consists of two molecules of pyridazine and one molecule of catechol (Figure 3.32) in the monoclinic space group  $P2_1/c$ . The catechol molecule is in the *anti-anti* conformation and hydrogen bonds to two pyridazine molecules to form a discrete ternary adduct. The most distinctive feature of this co-crystal is that not all N hydrogen bond acceptor sites are utilised by the strong donor atoms. These acceptor sites, instead, are involved in weaker C–H $\cdots$ N hydrogen bonding with one of the remote carbon atoms of an adjacent pyridazine molecule. Figure 3.33 illustrates this interaction as well as the C–H $\cdots$  $\pi$  interactions between the pyridazine and catechol molecules. Pyridazine molecules at either end of the adduct  $\pi\cdots\pi$  stack in an offset manner with neighbouring adducts. These weak interactions organise adducts into weakly associated wave-like chains (Figure 3.34). Weak C–H $\cdots$ O associations align catechol molecules along [001], such that alternating ‘chains’ are aligned in opposite directions along (100) (Figure 3.34)

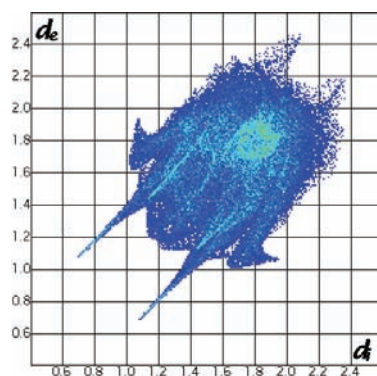


**Figure 3.33** Yellow arrows indicate C–H $\cdots$ O interactions and green arrows indicate C–H $\cdots$ N overlap. Surrounding molecules have been omitted for clarity.

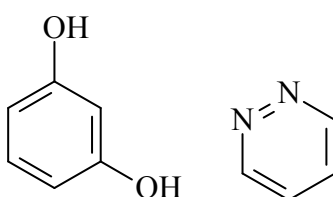


**Figure 3.34** Packing diagram of  $\beta$ -O<sub>2</sub>N<sub>2</sub> viewed along [001]. The orange shaded area highlights hydroxyl groups pointing towards the viewer and the blue area shows them pointing away.

The fingerprint plot (Figure 3.35) of  $\beta$ -O<sub>2</sub>N<sub>2</sub> provides an excellent example of recognizing distinctive intermolecular interactions. The directional O–H $\cdots$ N interactions are clearly indicated by the tails approaching 1 Å on both axes; C–H $\cdots$  $\pi$  interactions are inferred from the wings on either side of the plot, while the light blue area at 1.8 Å on the diagonal shows  $\pi$  $\cdots$  $\pi$  stacking in the structure.

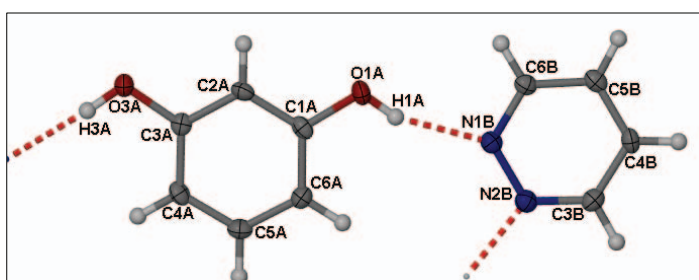
Figure 3.35 Fingerprint plot of  $\beta$ -O<sub>2</sub>N<sub>2</sub>

### 3.2.2 O<sub>3</sub>N<sub>2</sub> – Resorcinol and Pyridazine (1:1 ratio)



Scheme 3.8 Co-crystal formers resorcinol and pyridazine

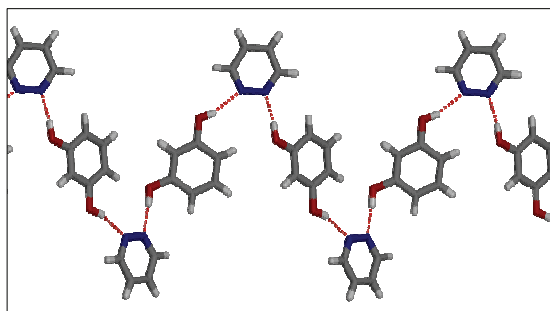
O<sub>3</sub>N<sub>2</sub> proved to be the most difficult co-crystal to obtain. Various solvents were employed as well as different techniques, including slow evaporation of solvent at room temperature, 4 °C and below freezing, solvent drop grinding (1:1, 1:2 and 2:1 ratios) and crystallization from the melt. On each occasion the result was the same – a reddish-brown oil. Single crystals were ultimately obtained from a 1:1 mixture of methanol and water, which was left to evaporate at room temperature.

Figure 3.36 Thermal ellipsoid plot of the ASU of O<sub>3</sub>N<sub>2</sub>

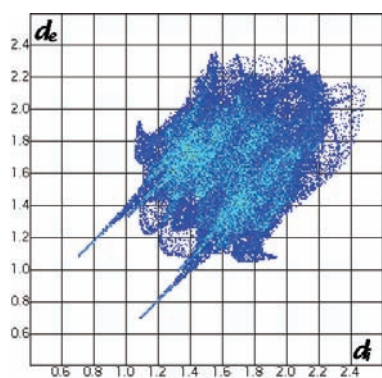
Resorcinol crystallises with pyridazine in the chiral space group,  $P2_12_12_1$ , with one molecule of resorcinol (*anti-anti*) and one molecule of pyridazine constituting the ASU (Figure 3.36). Hydrogen bonds form between the two

complementary molecules to form S-shaped chains,  $C_2^2(9)$  (Figure 3.37). Resorcinol adopts the *anti-anti* conformation in the structure of O<sub>3</sub>N<sub>2</sub>, which appears to cause one of the O–H $\cdots$ N interactions to be somewhat distorted (angle of 160(2)°).



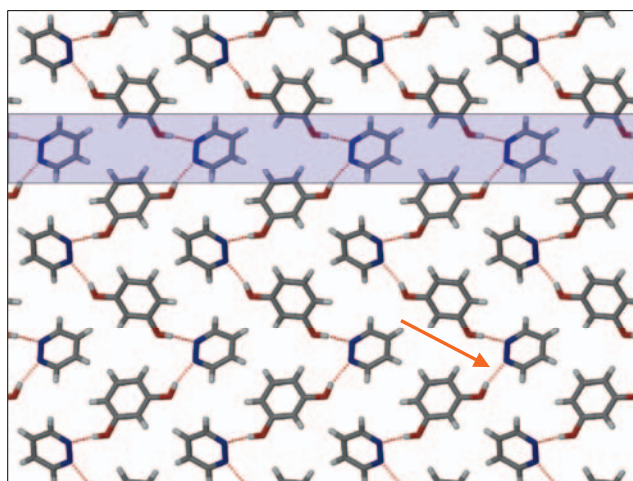


**Figure 3.37** A single S-shaped chain formed by strong hydrogen bonds between molecules of O3N2.



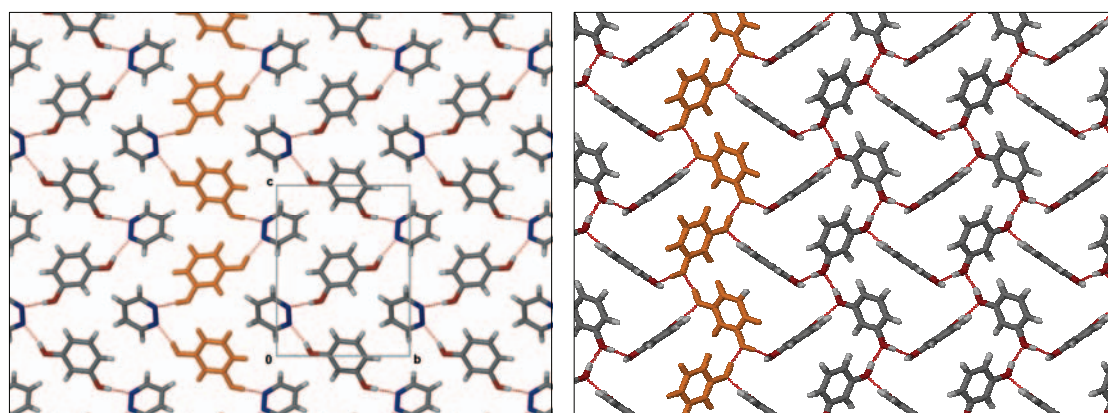
**Figure 3.38** Fingerprint plot of O3N2

The fingerprint plot (Figure 3.38) for O3N2 highlights the existence of C–H $\cdots$  $\pi$  interactions (wings) between molecules, while C–H $\cdots$ O interactions are shown by the shorter inner tails that are slightly obscured by the longer outer tails characteristic of the O–H $\cdots$ N hydrogen bonds. Hydrogen bonded chains are brought into close proximity by the C–H $\cdots$ O interactions between symmetry-related resorcinol molecules within the same chain. This interaction results in puckering of the chains (Figure 3.39). The puckering allows adjacent chains to slot into one another by means of C–H $\cdots$ O interactions between pyridazine and resorcinol molecules of neighbouring chains, resulting in a 2-D layer parallel to the *bc* plane. The pyridazine of one chain is positioned between two resorcinol molecules of another, allowing C–H $\cdots$  $\pi$  and lone-pair $\cdots$  $\pi$  interactions. Chains fit into one another such that pyridazine molecules are aligned in the same direction (along [010]) to form a 2-D layer. Layers then pack in an ABAB fashion along the *a* axis to overlay any void spaces created within a layer. This aggregation is supported by numerous C–H $\cdots$ N contacts between the layers.



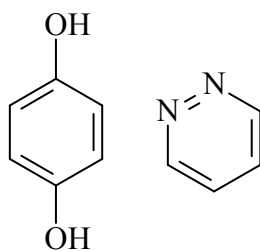
**Figure 3.39** A single hydrogen bonded layer of O3N2. The area shaded blue illustrates the pyridazine molecules aligned in one direction. The orange arrow indicates the distorted H-bond.

The structure of O3N2 displays similarities in arrangement of resorcinol molecules to those in the single-component resorcinol (O3) (Figure 3.40). Thus, it is plausible that the pyridazine molecules simply embed themselves into the resorcinol array replacing “redundant” resorcinol molecules and forming O–H····N hydrogen bonds. Resorcinol molecules in O3N2 correspond to those of the single-component resorcinol structure, with a slight shift of the molecules to accommodate hydrogen bonding to pyridazine. It is interesting that the resorcinol molecules would opt to form the co-crystal compound as there are fewer strong hydrogen bonds (O3N2) sustaining the 3-D structure. However, there is a slight gain in density for the binary crystal ( $1.36 \text{ g cm}^{-3}$  for O3N2;  $1.31 \text{ g cm}^{-3}$  for O3). This could provide an explanation for why the crystals of O3N2 were difficult to grow in the first place. Reference is again made to this structure in Section 3.2.3.

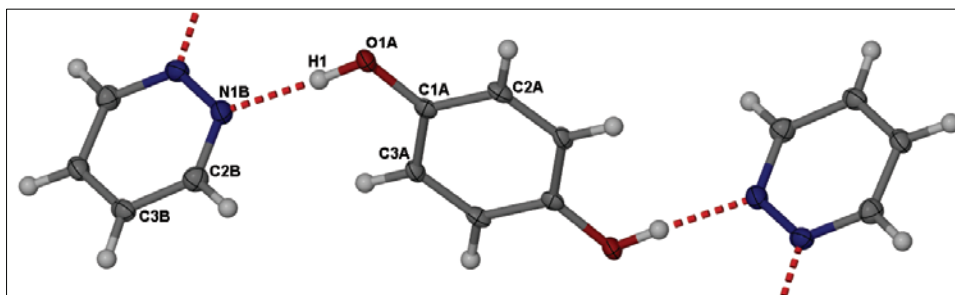


**Figure 3.40** Comparison of the resorcinol molecules in co-crystal O3N2 (left), highlighted in orange, with the arrangement of the same molecule in the starting material (RESORA03) (right)

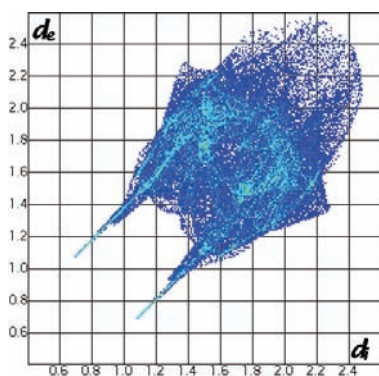
## 3.2.3 O4N2 – Hydroquinone and pyridazine (1:1 and 1:2 ratios)



Scheme 3.9 Co-crystal formers hydroquinone and pyridazine

 $\alpha$ -O4N2 (1:1)Figure 3.41 Thermal ellipsoid plot of the ASU of co-crystal  $\alpha$ -O4N2. ASU atoms are labelled.

The  $\alpha$ -O4N2 form crystallises in the monoclinic space group  $C2/c$  with half a molecule of each component in the ASU (Figure 3.41). Hydroquinone is situated on an inversion centre  $(\frac{1}{2}, \frac{3}{4}, 0)$  and pyridazine is located on a diad  $(\frac{1}{2}, y, \frac{1}{4})$ .

Figure 3.42 Fingerprint plot of  $\alpha$ -O4N2

Hydroquinone H-bonds to the pyridazine molecule *via* the  $O-H \cdots N_{\text{arom}}$  synthon to form a 1-D zigzag polymeric chain. These chains are retained in position by  $C-H \cdots O$  interactions between the remote carbon of the pyridazine molecule and oxygen of the hydroquinone, thus organising the chains into layers as shown in Figure 3.43 (left). Layers alternate in an ABAB manner along [001] such that alternate layers are rotated  $180^\circ$  with respect to each other and chains form a criss-cross pattern. This arrangement facilitates lone-pair  $\cdots \pi$  interactions between hydroxyl groups and pyridazine rings of separate layers. The fingerprint plot of  $\alpha$ -O4N2 (Figure 3.42) supports this observation, with long outer tails for the  $O-H \cdots N$  hydrogen bonds. The shorter inner tails, shown as a broadening of the  $O-H \cdots N$  tails, indicate the  $C-H \cdots O$  interactions.

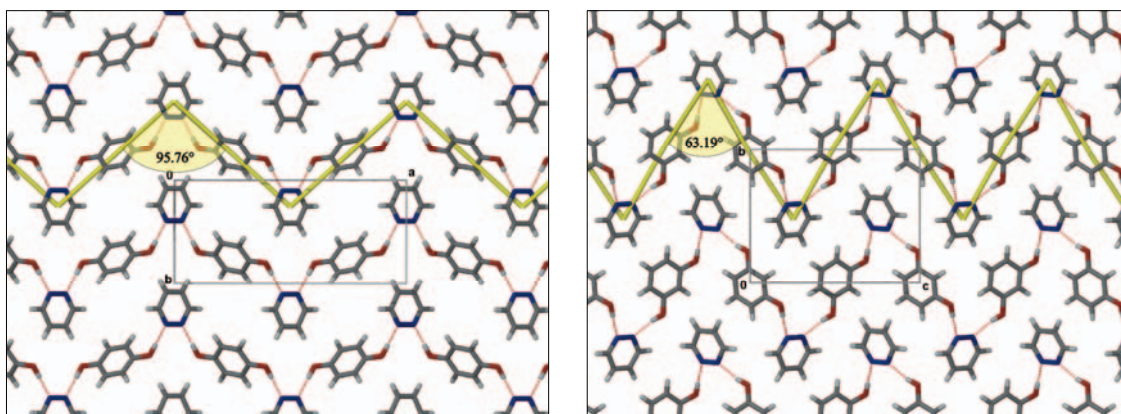


**Figure 3.43** Representations of a single layer of the structures  $\alpha$ -O4N2 (viewed down [001]) on the left and O3N2 (viewed down [100]) on the right. Comparison of the two clearly shows the difference in chain angles caused by positional switching of the hydroxyl group from the *meta*- (O3N2) to *para*-position ( $\alpha$ -O4N2).

Remarkable similarities exist between the structures of O3N2 and  $\alpha$ -O4N2 (Figure 3.43). This is an interesting occurrence since the positions of the hydrogen bond donors are thought to be important factors in the outcome of the structure. In these structures the *meta* and *para* positioning of the donors result in similar 1:1 H-bonded polymeric chains. The proximity of the two hydroxyl groups to each other in the benzenediol isomers does not bring about a large change in the actual arrangement of the 2-D layer, although the geometrical parameters within the layers differ. One of the visibly different aspects when viewing the two structures in Figure 3.43 is the angle produced by the hydrogen bonded 1-D chains as well as the rotation of the hydroxyl groups in relation to the aromatic ring moiety. The hydrogen bonded chain in  $\alpha$ -O4N2 subtends an angle of  $95.8^\circ$  which is less angular than in O3N2 ( $63.2^\circ$ ). The hydroquinone molecule ( $\alpha$ -O4N2, *para*) is rotated to almost  $90^\circ$  relative to the plane projected by the pyridazine molecules, while resorcinol (O3N2, *meta*) remains relatively planar with a slight twist to accommodate the *meta* positioning of the donor atoms. Pyridazine rings are arranged in a similar manner in both structures – along a column the molecules are aligned in the same direction (along *b* axis in both structures) while rows alternate (along *a* axis in  $\alpha$ -O4N2 and along *c* axis in O3N2).

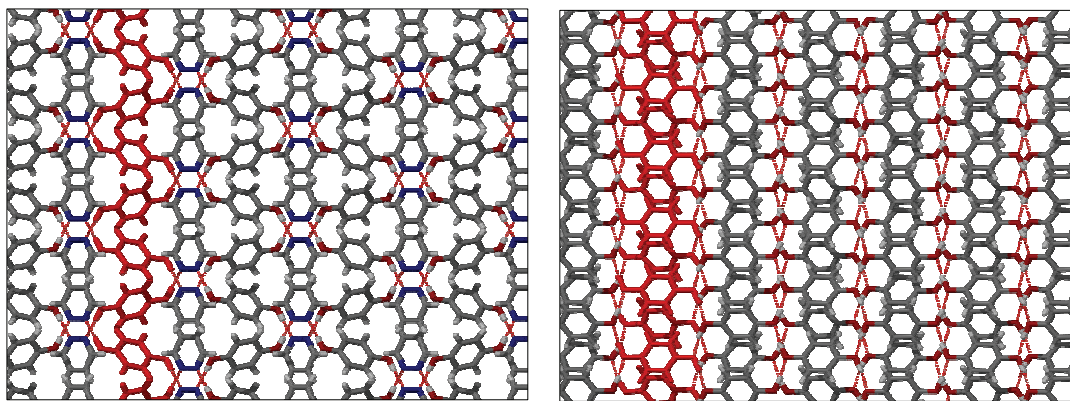


**Figure 3.44** Comparison of co-crystal  $\alpha$ -O4N2 (left) with the  $\gamma$ -form of hydroquinone (right). Two alternating layers are displayed to allow pattern comparison

The structure of co-crystal  $\alpha$ -O4N2 is also comparable to that of the  $\gamma$ -form of hydroquinone (Figure 3.44). There are clear differences between the two structures since one consists of only one-component while the other contains a second distinct molecule that can hydrogen bond in a different manner. However, when the hydrogen bonding pattern is overlooked, the positioning of the molecules is similar. It could be speculated that the pyridazine molecules are able to replace alternating columns of hydroquinone molecules in favour of forming the O–H $\cdots$ N hydrogen bond.

PXRD analysis (Figure 3.46) of the solid product formed in a SDG experiment of a 2:1 ratio of hydroquinone to pyridazine yields a near perfect match to the simulated pattern of  $\alpha$ -O4N2. It was determined that if the diol is added in excess, the  $\alpha$ -form results, while an excess of the diazine results in the  $\beta$ -form (discussed in the section below). A DSC trace of  $\alpha$ -O4N2 (Figure 3.45) reveals a single thermal event with  $T_{\text{on}}=83$  °C.

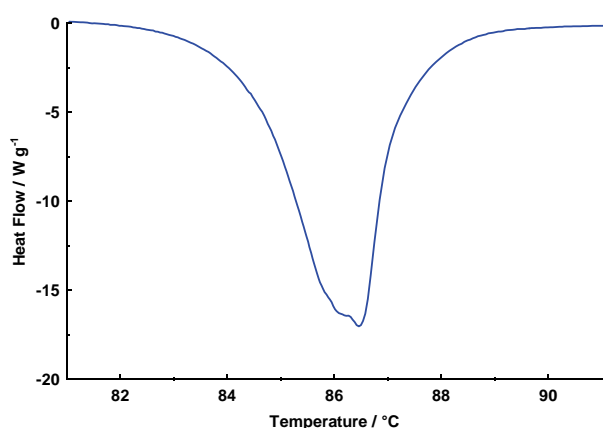


**Figure 3.45** DSC trace of  $\alpha$ -O4N2 product from the SDG experiment.



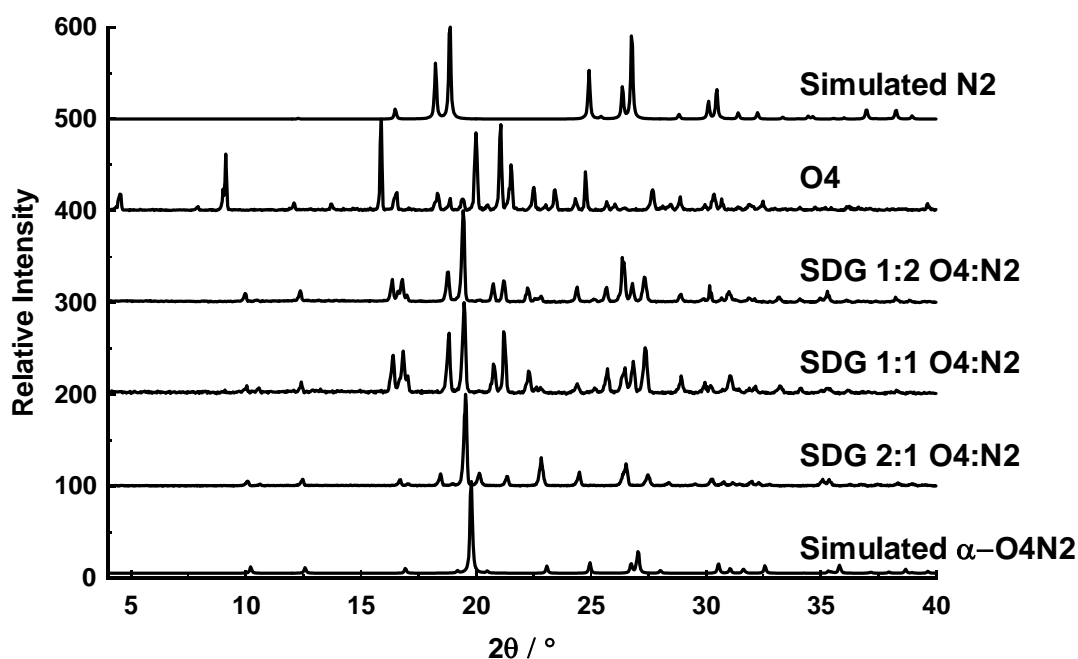


Figure 3.46 PXRD comparison of the SDG experiments with the simulated pattern of  $\alpha$ -O4N2.

### $\beta$ -O4N2 (1:2)

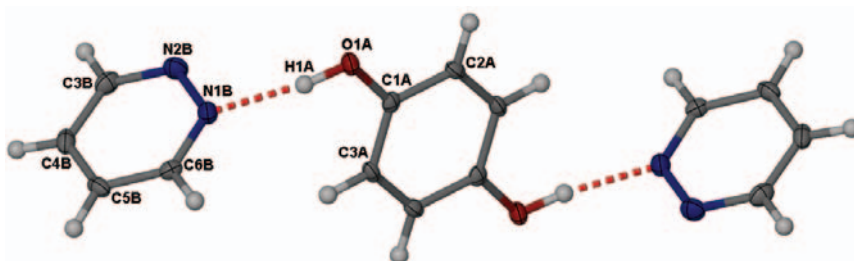
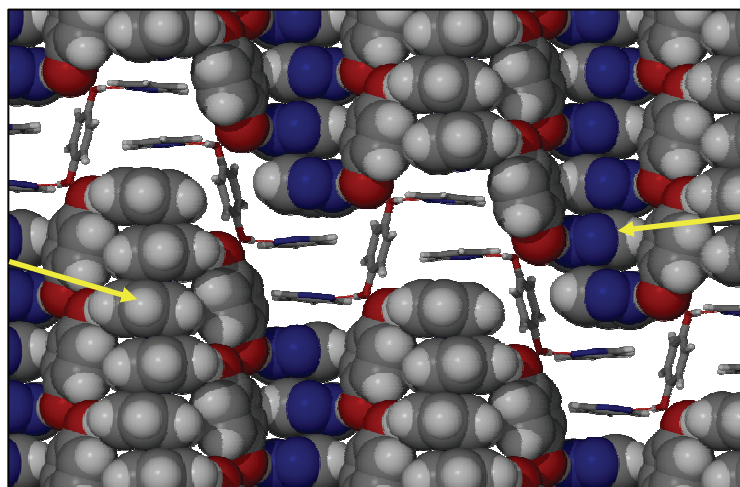


Figure 3.47 Thermal ellipsoid plot of ASU of  $\beta$ -O4N2. ASU atoms are labelled.

Ordinarily one would assume that all potential H-bond formers would be employed in the creation of a multi-component crystal (according to Etter's guidelines<sup>16</sup> as described in Chapter 1) so it is unusual, but not uncommon, that we find structures in which all possible H-bonds are not formed. An example would be the structure obtained concomitantly with  $\alpha$ -O4N2 from a 1:1 solution of hydroquinone and pyridazine. The  $\beta$ -O4N2 structure forms discrete ternary adducts, in place of the expected 1:1 association seen in  $\alpha$ -O4N2.

In this structure the pyridazine molecule only allows one of its nitrogen atoms to take part in hydrogen bonding with the hydroquinone molecule (Figure 3.47). The second potential H-bonding site is obstructed by an adjacent adduct, positioned to promote C-H $\cdots$ N interactions between a remote carbon atom and the nitrogen atom of a neighbouring pyridazine. Ternary adducts are assembled in a near-chair conformation (pyridazine molecules *anti* to each other). The packing arrangement of these chairs is such that the

pyridazine rings of alternate adducts stack (Figure 3.48), leading to a close-packed structure that is denser ( $1.374 \text{ g cm}^{-3}$ ) than  $\alpha\text{-O4N2}$  ( $1.338 \text{ g cm}^{-3}$ ).



**Figure 3.48** A packing diagram showing the chair conformation (stick representation) adopted by ternary adducts of  $\beta\text{-O4N2}$ . The space-fill molecules illustrate the stacking of pyridazine molecules into *anti*-parallel columns (indicated by arrows).

The fingerprint plot (Figure 3.49, left) shows the characteristic O–H $\cdots$ N tails, used in hydrogen bonding, as well as C–H $\cdots$  $\pi$  interactions (wings) between pyridazine and hydroquinone of neighbouring adducts. Details of these weaker interactions are found in Table 3.3 in the Appendices. This fingerprint plot bears striking similarity to that of  $\beta\text{-O2N2}$  (Figure 3.49, right), which is indicative of the similar packing arrangement of the two structures (Figure 3.50).

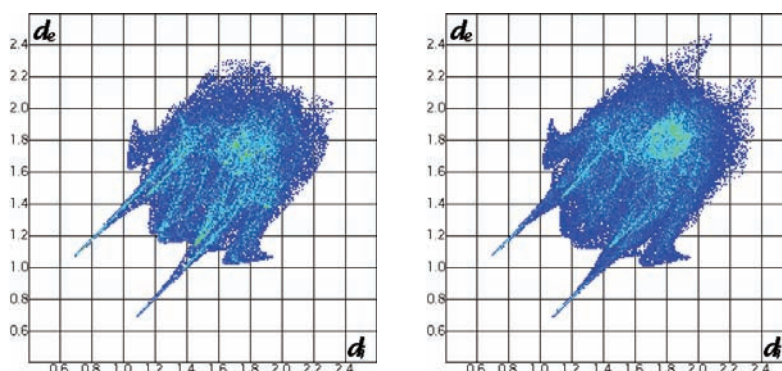


**Figure 3.49** Fingerprint plots of  $\beta\text{-O4N2}$  (left) and  $\beta\text{-O2N2}$  (right).

The difference in the arrangement in the third dimension of these two structures is probably because hydroquinone does not have the potential for polar alignment, whereas catechol does. The mode in which adducts form in  $\beta\text{-O4N2}$  generates *anti*-parallel columns of pyridazine stacks within a layer (face in opposite directions, Figure 3.48) brought about by the H-bonding with hydroquinone (*trans*-conformation).

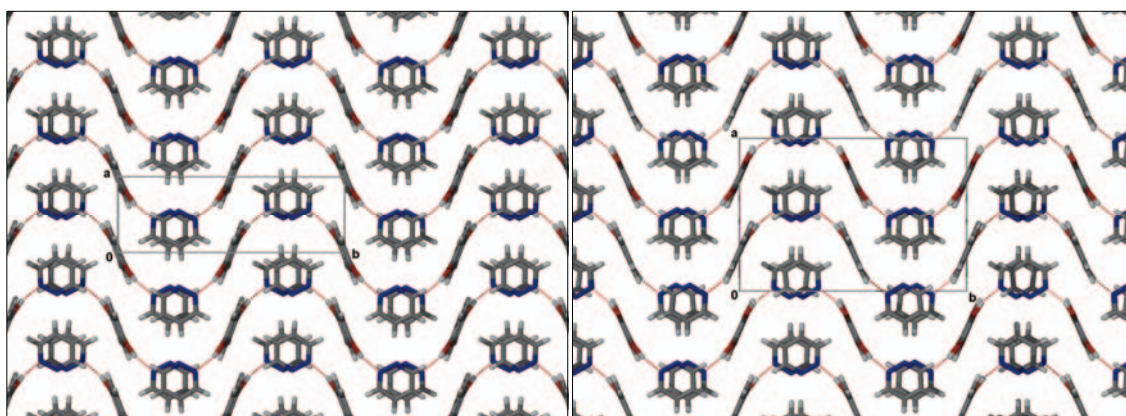


**Figure 3.50** Packing diagrams of  $\beta$ -O4N2 (left) and  $\beta$ -O2N2 (right), both viewed along [001].

The PXRD pattern for the bulk material, from which the single crystal of  $\beta$ -O4N2 was selected, is comparable to the pattern simulated from  $\alpha$ -O4N2 data. This is because the two structures of O4N2 were obtained concomitantly, but  $\beta$ -O4N2 constitutes the minority (Figure 3.51). However, the diffractogram obtained from a SDG experiment, carried out with a 1:2 ratio of hydroquinone to pyridazine, is a close match to the simulated pattern of  $\beta$ -O4N2 if temperature effects are taken into account.

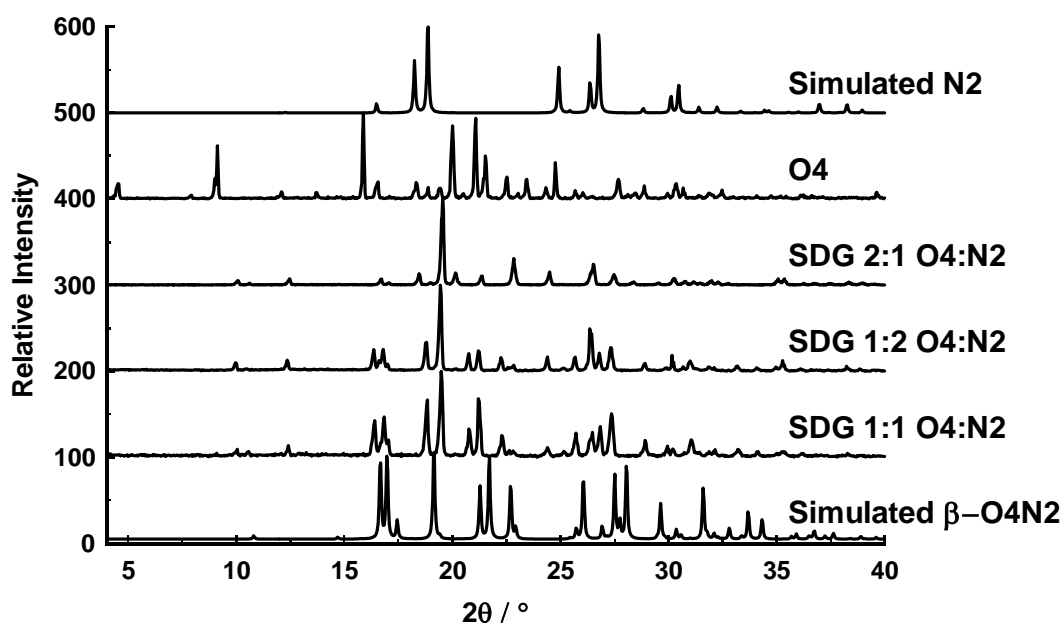


**Figure 3.51** PXRD comparison of the product of three SDG experiments with the simulated pattern of  $\beta$ -O4N2 and the two pure components pyridazine and hydroquinone.

The DSC trace for the SDG product shows a thermal event ( $T_{on}$ ) at approximately 81 °C with different peak shapes in cycles 1 and 2 (Figure 3.52). The bump in the event of the second cycle is possibly due to the transformation of the  $\beta$ -O4N2 to  $\alpha$ -O4N2 (variable temperature PXRD is required to confirm this). Therefore, it can be said that the  $\alpha$ -O4N2 is the more thermally stable of the two forms and is thus the thermodynamic product of



crystallisation. This explains why the PXRD of the bulk material matches the simulated pattern of  $\alpha$ -O4N2.

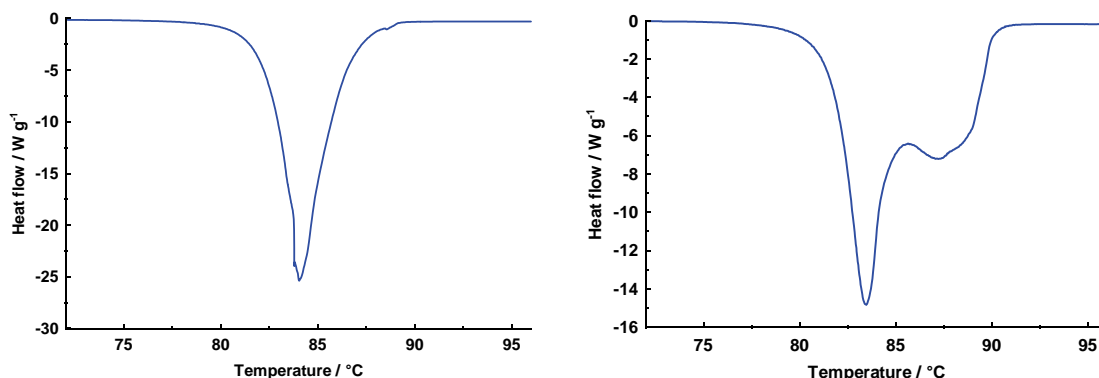
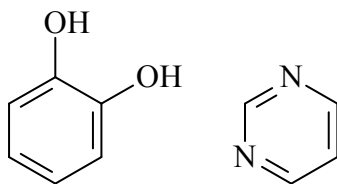


**Figure 3.52** DSC trace for  $\beta$ -O4N2. The first cycle (left) shows a single phase transition,  $T_{\text{on}} = 81$  °C, the second cycle (right) shows two closely related events,  $T_{\text{on}} = 81$  °C and at 85 °C.

Theoretical calculations were performed to determine which structure would assemble preferentially based on energy minimisations. It was determined that the structure of  $\alpha$ -O4N2 is slightly lower in energy ( $0.7 \text{ kcal mol}^{-1}$ ) owing to the slightly staggered hydrogen atom of the hydroxyl group of hydroquinone. Different interactions are involved in the construction of the resulting assemblies. The structure of  $\alpha$ -O4N2 makes use of  $\text{O-H}\cdots\text{N}$  and  $\text{C-H}\cdots\text{O}$  interactions as stated previously, with the  $\text{O-H}\cdots\text{N}$  bond strength being in the order of  $7.6 \text{ kcal mol}^{-1}$ , typical of a hydrogen bond. The  $\text{C-H}\cdots\text{O}$  interactions, however, are repulsive in nature, thereby destabilising the system by approximately  $1.8 \text{ kcal mol}^{-1}$  each.

In  $\beta$ -O4N2, the  $\text{O-H}\cdots\text{N}$  bond is marginally weaker than that found in  $\alpha$ -O4N2 ( $6.9 \text{ kcal mol}^{-1}$ ) but molecules are oriented such that  $\text{C-H}\cdots\pi$  interactions are attractive and stabilise the system by  $1.4 \text{ kcal mol}^{-1}$  each. However,  $\pi\cdots\pi$  interactions between the pyridazine molecules are weakly repulsive, destabilising the system by  $0.9 \text{ kcal mol}^{-1}$ . Thus in a model system of four molecules each of hydroquinone and pyridazine, it is found that  $\alpha$ -O4N2 is energetically more stable than  $\beta$ -O4N2.

### 3.2.4 O2N3 Catechol and pyrimidine



**Scheme 3.10** Co-crystal formers catechol and pyrimidine

## O2N3 (1:1)

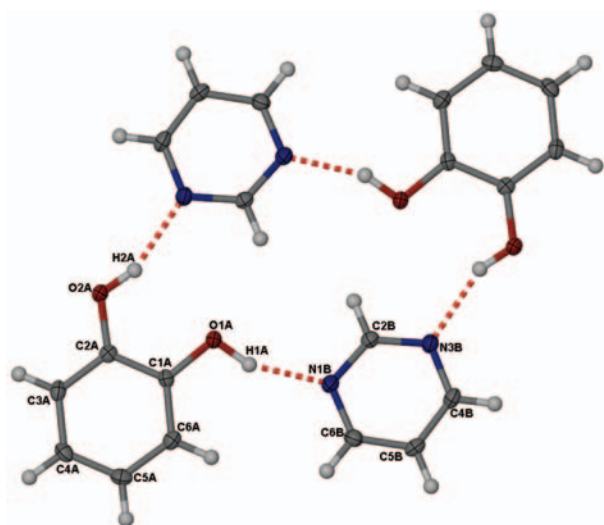


**Figure 3.53** Thermal ellipsoid plot of a quaternary adduct of O2N3. The ASU is labelled.

O2N3 crystallises in the monoclinic space group  $P2_1/c$  with an entire molecule of each of the starting materials in the ASU (Figure 3.53). Catechol and pyrimidine form an approximately planar quaternary adduct by utilising all possible H-bond donors and acceptors. Hydroxyl groups of the catechol molecule adopt the *syn-anti* conformation for formation of the discrete aggregate. Adducts form layers perpendicular to  $[-101]$ , held together by C–H $\cdots$ O interactions between pyrimidine and

catechol and these layers pack in a herringbone motif (Figure 3.54) along the  $b$  axis.

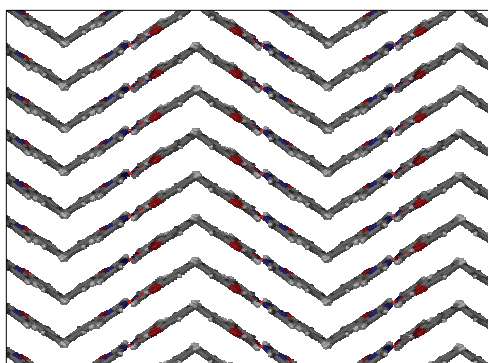


**Figure 3.54** Packing of O2N3 viewed down  $[-101]$  to show the herringbone motif.

The fingerprint plot (Figure 3.55, left) illustrates the intermolecular interactions present in O2N3. The longer, outer tails indicate use of the O–H $\cdots$ N synthon, while inner tails (Figure 3.55, right) show the C–H $\cdots$ O interactions and the green area on the diagonal (1.7 Å) depicts weak  $\pi\cdots\pi$  interactions between pyridazine rings.

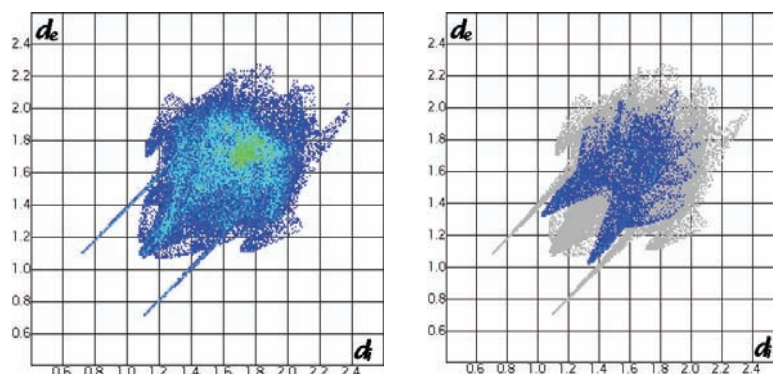


**Figure 3.55** Fingerprint plot of co-crystal O2N3 (left). The plot on the right indicates C–H····O interactions.

The PXRD pattern obtained from SDG experiments is comparable to that simulated from single-crystal data of O2N3 (Figure 3.56). An excess amount of pyrimidine appears to have no effect on the outcome of the experiment. An oily product formed during the SDG of the 2:1 ratio and this product, therefore, could not be analysed by PXRD. The SDG products shows that a residual amount of catechol is still present. The peak positions of the simulated pattern, especially at high  $2\theta$  angles, are shifted slightly to the right owing to the low temperature SCD data collection. The DSC trace (Figure 3.57) shows two thermal events, suggesting the existence of another form of the O2N3 co-crystal. The first cycle shows the first thermal event ( $T_{\text{on}} = 44\text{ }^{\circ}\text{C}$ ) as only a small bump with the second event being somewhat more intense ( $T = 66\text{ }^{\circ}\text{C}$ ). The second cycle, however, shows the two events having similar intensities. This may be indicative of a kinetic product of crystallisation at  $66\text{ }^{\circ}\text{C}$  and a thermodynamic product of crystallisation at  $44\text{ }^{\circ}\text{C}$ . These two forms, if they exist, may be in different molecular ratios. Further investigation by variable temperature PXRD is required to determine the molar ratio of the two phases.

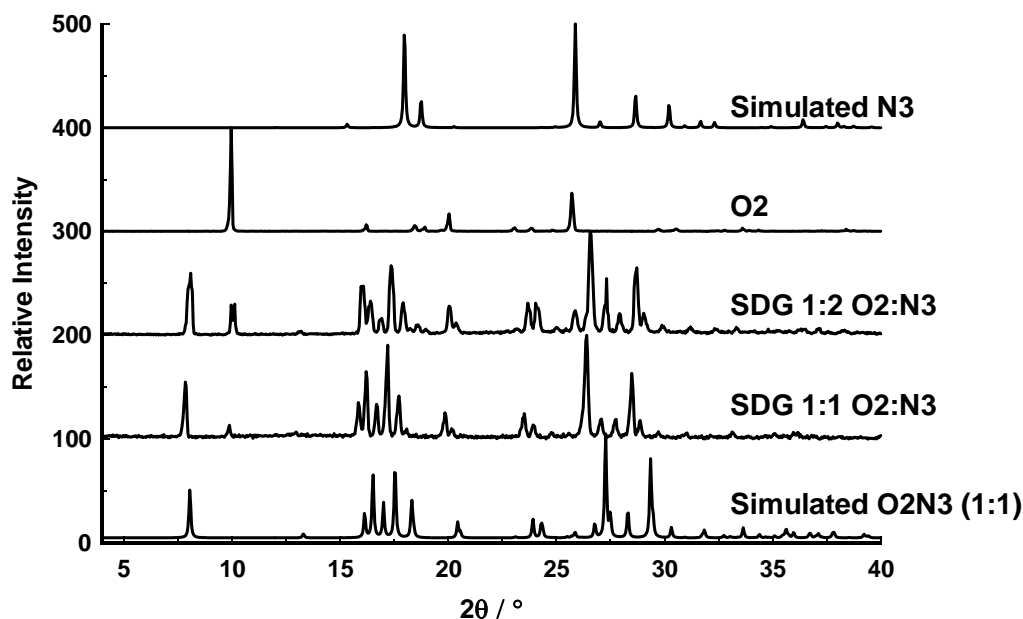


**Figure 3.56** PXR D comparison of the 1:1 and 1:2 SDG products with the simulated pattern of O2N3 and the two pure components pyrimidine and catechol.

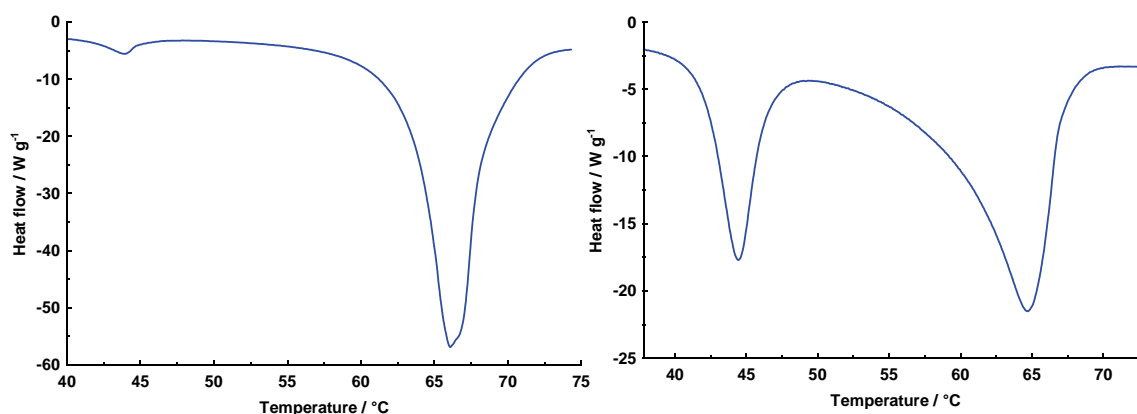
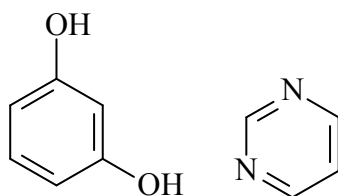


**Figure 3.57** DSC trace of O2N3 (SDG) of the first cycle of thermal procedure (left) with one intense event at 66 °C and a smaller minor event at 44 °C. The second cycle (right) shows the two events with similar intensities.

### 3.2.5 O3N3 – Resorcinol and pyrimidine (1:1 and 2:1 ratios)



**Scheme 3.11** Co-crystal formers resorcinol and pyrimidine

Numerous attempts were made to obtain a co-crystal of the above materials. Both structures reported here are unstable at room temperature and melt rapidly on removal from the cold N<sub>2</sub> stream of the diffractometer.